

DESIGN AND FABRICATION OF AN AUTOMOBILE

DISK BRAKE BALANCING MACHINE

A final year project report

Presented to

SCHOOL OF MECHANICAL AND MANUFACTURING ENGINEERING

Department of Mechanical Engineering

NUST

ISLAMABAD, PAKISTAN

In Partial Fulfillment
of the Requirements for the Degree of
Bachelors of Mechanical Engineering

by

Farhan Ellahi

Gohar Shoukat

Usama Zaid Malik

June 2017

EXAMINATION COMMITTEE

We hereby recommend that the final year project prepared under our supervision by Farhan Ellahi (NUST201304475B11113F), Gohar Shoukat (NUST201305490B11113F) and Usama Zaid Malik (NUST201304802B11113F) for the project titled “Design and fabrication of an automobile disk brake balancing machine” be accepted in partial fulfillment of the requirements for the award of Bachelors of Engineering in Mechanical degree.

Supervisor: Dr. Riaz Ahmed Mufti, Professor Department of Mechanical Engineering	_____
	Dated: _____
Committee Member: Dr Samiur Rahman Shah, Assistant Professor, Department of Mechanical Engineering	_____
	Dated: _____
Committee Member: Dr. Mian Ashfaq Ali Assistant Professor Department of Mechanical Engineering	_____
	Dated: _____

(Head of Department)

(Date)

COUNTERSIGNED

Dated: _____

(Dean / Principal)

ABSTRACT

The Design of an Automobile Disk Brake Balancing Machine was chosen as the final year project by the aforementioned team. The scope of this work involves the design and fabrication of non-rotating static disk brake balancing machine. The project was undertaken as a proof of concept for the industry partner, MECAS Engineering, which aims to introduce this as a regular feature for its product line.

The concept design for the project was unconventional. The design team opted for a non-rotational balancing machine instead of the renowned rotational ones. This decision was taken after a thorough analysis of several rotational and non-rotational designs and eventually based on a design selection matrix.

The non-rotational machine employs three equally spaced load-cells which measure the weight distribution of the disk brake positioned on top, instead of measuring the vibration of the rotor during rotation. The array of data from each of the load-cells was filtered, processed and finally integrated with each other to obtain meaningful information about the location and mass of unbalance. The minimum unbalance detection of 1300 gmm which was the limit set by the industry partner was successfully achieved with strict conformity with ISO 1940-1:2003 balancing quality standards for grade 40 rotors.

By removing rotational components, the machine has practically eliminated any chances of injury. It also comes with a more economic price tag and substantially reduces cycle time for increased inspection rates. The graphical user interface made by using LabVIEW assists a common every day worker in easy operation and maintainability of the machine and its software architecture.

PREFACE

School of Mechanical and Manufacturing Engineering has been striving to connect with the industry and solve its problems. To serve the mission, several industrial projects have been proposed and delivered in the past. Among the projects, balancing machines have been in high demand. A disk brake balancing machine based on the rotational design using motors and vibration sensors was manufactured in collaboration with Hybrid Engineering. Our project is a continuation and extension to the existing machine.

ACKNOWLEDGMENTS

The authors of this report would like to thank School of Mechanical and Manufacturing Engineering for providing them with the opportunity to express their knowledge practically and enhance their technical as well as soft skills on every step of the project. It mustn't go out of notice that the authors understand the shortcomings within the system and really appreciate the steps taken by the department as a whole to improve the quality of the projects. Professor Abdul Ghafoor must be appreciated for empowering his team to take the necessary steps to make the changes necessary.

The authors want to thank the school for making available DICE office for their use without interruption and Dr Jawad Aslam for the allowing the use of the office, even though it had been allocated to him months earlier.

The efforts of Zaid Ahsan Shah to go out of his way to help them deserves special mention here. He spent several hours trying to explain how to read data sheets and avoid errors in signal processing. Use of RISE Lab as a worksite for electronics also is acknowledged.

Sir Faisal at MRC and the extremely skillful welders at the Mehrabadi road played a crucial role in the manufacturing of the frame, especially, during the construction of the second prototype was in process. These individuals were often asked to put in hours first welding the frame and then grinding off the welds and redoing the entire structure again. They did it without ever complaining, even though, at times the frustration was pretty evident.

The project supervisor Dr Riaz Ahmed Mufti is thanked dearly for providing the authors with the project and enabling them to make the necessary decisions on their own discretion and encouraging them throughout the process with his carrot and stick approach.

Dr Aamir Mubasher and Dr Sami Ur Rehman Shah, the two other pillars of this project are appreciated for help and assistance. Their help and guidance was not only limited to technical assistance with the project, but spanned over personal and professional lives of the authors.

Lecturer Hafiz Abd-ur-Rehman, lead FYP coordinator, needs a special mention for his efforts to revive the culture of timely and effective check and balance throughout the course of the project. We are grateful to all management and faculty who supported him with the evaluation of projects.

Mr. Rizwan from Strongman Industries has proven to be a great help. His generous advice and donation of linear actuator with all its accessories was a valuable contribution for successful completion of this project. The authors are thankful to him for taking a keen interest in their work and supporting them, more than what was requested.

Talha Yousuf, a fellow batch mate is also thanked dearly for his efforts in assisting the authors with the various issues that came up time to time with the sensor integration with LabVIEW.

In the last, the project could never have been completed without the prayers and support of the families of the authors. Quite often, it wasn't just the mothers of the authors praying, rather the entire extended families which speaks loads about the importance each family associated with the final year project.

Dedicated to our families.

ORIGINALITY REPORT

Design and fabrication of an automobile disk brake balancing machine

ORIGINALITY REPORT

%9	%8	%3	%6
SIMILARITY INDEX	INTERNET SOURCES	PUBLICATIONS	STUDENT PAPERS

PRIMARY SOURCES

1	www.hep.man.ac.uk Internet Source	%3
2	hobbydistrict.com Internet Source	%2
3	Shiau, T. N., E. K. Lee, Y. C. Chen, and T. H. Young. "Dynamic Response of a Geared Rotor-Bearing System Under Residual Shaft Bow Effect", Volume 5 Marine Microturbines and Small Turbomachinery Oil and Gas Applications Structures and Dynamics Parts A and B, 2006. Publication	<%1
4	Submitted to Universiti Teknikal Malaysia Melaka Student Paper	<%1
5	www.amazon.com Internet Source	<%1
6	Yungong, Li, Zhang Jinping, Wang Liqiang, and Chen Yang. "A fault feature extraction method	<%1

for rotor rubbing based on load identification and measured impact response", *Procedia Engineering*, 2011.

Publication

7	doiserbia.nb.rs Internet Source	<% 1
8	Submitted to Franklin University Student Paper	<% 1
9	Submitted to LNM Institute of Information Technology Student Paper	<% 1
10	Submitted to Middlesbrough College Student Paper	<% 1
11	RICHARD E. BARLOW. International Journal of Reliability Quality and Safety Engineering, 1999 Publication	<% 1
12	bradscholars.brad.ac.uk Internet Source	<% 1
13	www.fastmodems.com Internet Source	<% 1
14	www.fishyfridays.com Internet Source	<% 1
15	d3s.mff.cuni.cz Internet Source	<% 1

16

espace.curtin.edu.au
Internet Source

<% 1

17

Johnson, G.L., and J.B. Martin. "The permanent deformation of a portal frame subjected to a transverse impulse", *International Journal of Solids and Structures*, 1969.
Publication

<% 1

18

Shiau, T. N., E. K. Lee, T. H. Young, and W. C. Hsu. "Dynamic Analysis of a Geared Rotor-Bearing System With Viscoelastic Supports Under the Bow Effect", *Volume 5 Turbo Expo 2007*, 2007.
Publication

<% 1

EXCLUDE QUOTES OFF
EXCLUDE BIBLIOGRAPHY OFF

EXCLUDE MATCHES OFF

COPYRIGHT

Copyright in test of this thesis with the student author. Copies (by any process) either in full or in extract may be only in accordance with the instructions given by the author and lodged in the library of SMME, NUST. Details may be obtained by the librarian. This page must be part of any such copies made. Further copies (by any process) of copies made in accordance with such instruction may not made without the permission (in writing) of the author.

The ownership of any intellectual property rights which may be described in this thesis us vested in SMME, NUST, subject to any prior agreement to the contrary, may not made available for the use of third parties without the written permission of SMME, NUST which will describe the terms and conditions of any such agreement.

Further information on the conditions under which disclosure and explanation may take place to available from the library of SMME, NUST Islamabad.

TABLE OF CONTENTS

ABSTRACT	iii
PREFACE	iv
ACKNOWLEDGMENTS	v
ORIGINALITY REPORT	viii
COPYRIGHT	xi
LIST OF FIGURES	xiv
NOMENCLATURE	xv
INTRODUCTION	1
Background	1
Project plan	2
Literature Review	4
METHODOLOGY	11
Working of the system	12
Mathematical equations and resulting imbalance	14
Manufacturing Eccentricity Compensation	15
Load cell uncertainty	16
Coding flowchart	18
RESULTS AND DISCUSSION	19
REFERENCES	24
APPENDIX I: LABVIEW USER INTERFACE	25

APPENDIX II: ISO STANDARD REFERENCE26

APPENDIX III: LOAD CELL DATA SHEET27

APPENDIX IV: BILL OF MATERIALS28

LIST OF FIGURES

Figure 1 Project timeline.....	2
Figure 2 Gantt chart (Microsoft project).....	3
Figure 3: Cracks on a disk Brake.....	4
Figure 4: CoR and CoG offset	5
Figure 5: In-plane Balancing	7
Figure 6: Dynamic Balancing	7
Figure 7: Disk Brake (Top), Gear (Bottom) and Grinding wheel (Right)	8
Figure 8: Force against angular velocity for different amounts of unbalance mass	9
Figure 9: Free Body Diagram of Disk Brake.....	14
Figure 10: Resultant imbalance due to eccentricity	15
Figure 11: coding steps	18
Figure 12: Unbalance values at different locations of known mass	19
Figure 13: Comparison of bearing given by machine with a known bearing.....	20
Figure 14: 90% Confidence Interval for the amount of unbalance.....	21
Figure 15: 90% Confidence Interval for the location of unbalance.....	21
Figure 16: Briiel & Kjaer Unbalance Nomogram, based on ISO quality standards.....	26

NOMENCLATURE

F	Force (N)
$\sum F = 0$	Summation of forces for equilibrium
θ	Theta, location of unbalance from a reference point (Degrees)
M_y	Moment about the y-axis (N.m)
r	Radius of unbalance from the geometrical center of the disk (m)
m	Amount of unbalance on the disk (kg)
g	Acceleration due to free fall (m/s^2)
W	Weight of Disk (N)

INTRODUCTION

Background

With the completion of the first leg of China Pakistan Economic Corridor in 2018, Pakistan will experience accelerated growth with higher living standards. The rejuvenated National Automotive Policy is a clear indicator. Transportation and personal vehicles will see rapid expansion. The announcement of major companies like Renault has already set the pace for post CPEC era in Pakistan.

MECAS Engineering, an industry partner of Hybrid Engineering with whom the team is collaborating for their final year project aims to induct this machine into their product line for speedy inspection, should it clear the extensive testing it is being subjected to. Hybrid Engineering has already issued a Letter of Support stating the viability of this project.

This machine is an example of the budding relationship that futuristic industries and academicians have in Pakistan. The machine will serve as a research bed for non-rotational and highly customized balancing machines.

Three load cells were used to measure the weight distribution and hence, any unbalance mass present within the rotor. The data from each load-cell was processed to give the final detail about the amount and location of unbalance. This data was processed through LabVIEW and a graphical user interface was developed for the ease of the operator.

Project plan

Project management was given due consideration. Various strategies were implemented as learned during courses along with help from experience in past projects and supervisor guidance.

Tools uses:

1. Microsoft project 2013 for planning and tracking progress of the project
2. Dropbox for file sharing and Microsoft OneNote for making notes
3. Email and Social media platforms for effective communication

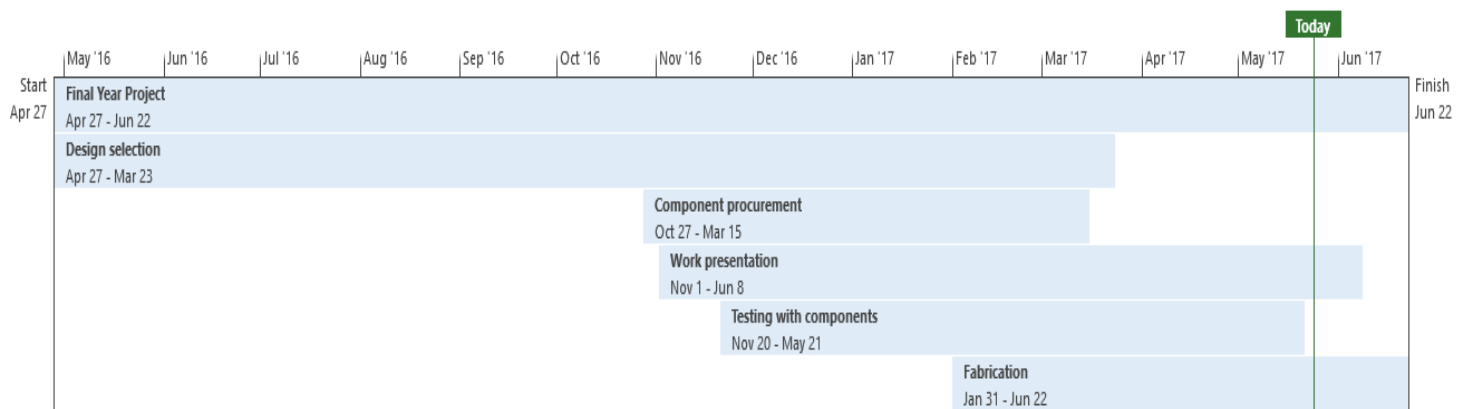


Figure 1: Project timeline¹

¹ Due to unplanned variations in working times, tracking of work hours was considered unpractical, so progress tracking was carried out by assigning deadlines through manual scheduling. Exam weeks as well as other predictable non-working days were incorporated in the working calendar of project management software.

Work breakdown structure and responsibility assignment

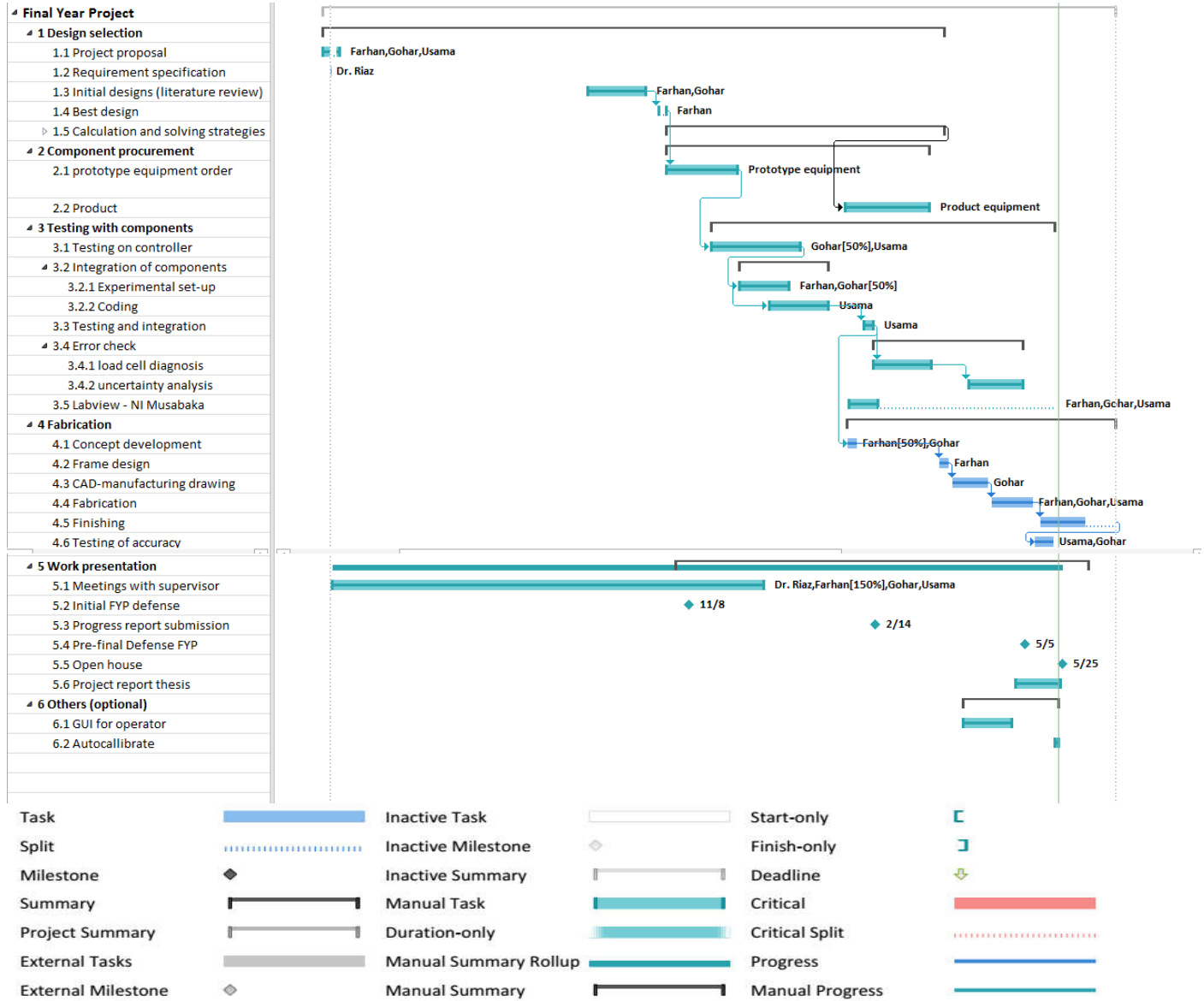


Figure 2: Gantt chart (Microsoft project)

LITERATURE REVIEW

Rotors are an essential feature of modern machinery. They are found in a multitude of machines, from the chuck of a lathe to the shaft of the jet engine that powers aircrafts. Their applications are as extensive as the variety of machinery they are found in – transferring torque, altering RPM or simply acting as a pulley.

These rotors, usually coupled with other machine parts like gear trains run at high RPMs. It is a common observation that as the RPM of a rotor increases, the vibrations and noise it produces, increases. If this vibration is not attended to, it can lead to machines malfunctioning. The situation is further aggravated when the rotor is subjected to high thermal stresses along with mechanical stresses[1, 2]. The thermal stress due to braking and mechanical fatigue caused by vibration can bring about a catastrophic failure resulting in significant financial loss. Mackin et al.[1] studied the disk brake behavior under high thermos-mechanical fatigue during high g braking. The analysis showed that this fatigue causes crack propagation through the rotor's thickness and along its radius. Boniardi et al.[3] studied motorcycle disk brakes to reach similar conclusions about the effect of thermos-mechanical fatigue on the life of disk brakes. The studies also revealed the concentration of cracks near the holes drilled through the disk for ventilation as shown in Figure 3.

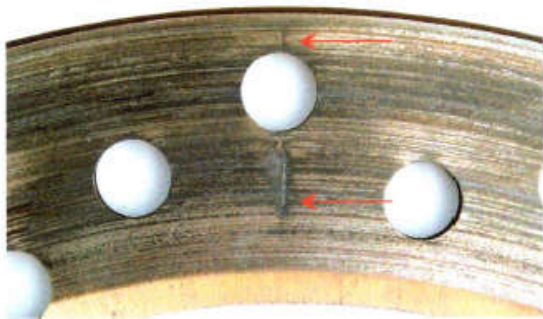


Figure 3: Cracks on a disk Brake

One of the leading causes of vibrations in rotors resulting in their failure can be attributed to the imbalance or residual mass present within the system[2, 4] . During rotation, unbalance generates centrifugal forces which in turn produce vibrations and noise. Tian et al.[4] worked on a compressor which vibrated significantly at high rpms, careful analysis showed presence of imbalance that had to be corrected before the compressor showed substantially reduced vibration levels. Choy and Tu.[5] concluded that mass imbalance significantly impacts the operational life and efficiency of rotors which necessitates the study of the impact of these imbalance induced vibrations on different rotors.

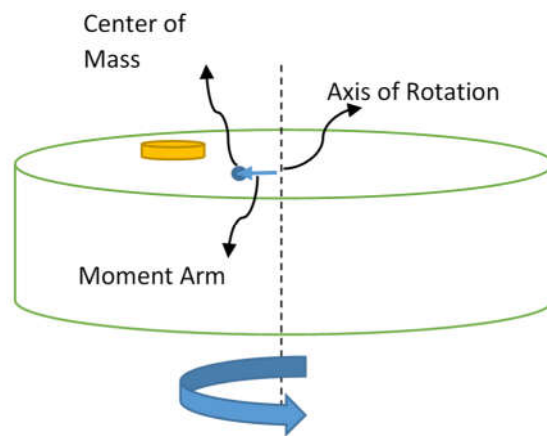


Figure 4: CoR and CoG offset

The existence of imbalance in a rotor can be due to several reasons, all of which create an offset between the center of mass of rotor and the axis of rotation, thereby providing a moment arm as indicated by Figure 4. This gives rise to centrifugal acceleration that is proportional to the square of the angular velocity. One of the leading causes of imbalance as Beatty [6] explained is the rubbing of high-speed, high-performance rotors with stationary parts like journal bearings which result in the uneven mass removal due to wear and tear from the surface in contact with the stationary part; manufacturing imperfections as Shortle and Mendel [7] argue also contribute significantly to residual imbalance within the rotor - geometrical imperfections like nicks and bumps on the surface may alter the

mass distribution of the rotor. Their study further went on to quantify the influence manufacturing processes like feed rate have on the imbalance. Their results led to the following equation which relates imbalance with the feed rate and speed of lathe:

$$E(\tau) \propto \sqrt{\frac{v}{w}} \quad \text{Equation 1}$$

Similar to the turning operation, processes like drilling, boring and welding too alter the mass distribution. Unbalanced rotors, regardless of how it is induced, are harmful for a system and can negatively affect system performance. In worst cases, result in catastrophic failure, leading to loss of property and life.

It is therefore imperative that the residual mass/unbalance is detected in a rotor before it is commissioned for use. This can be further divided into two categories based on the geometric thickness of the rotor- static balancing and dynamic balancing. As per Equation 2, if the axial dimension H is smaller compared to the diameter D, the rotor is considered to be disk like.

$$\frac{B}{D} > 0.2 \quad \text{Equation 2}$$

It is reasonable to estimate that the mass of such rotors lie in a common transverse plane[8]. Common examples of such rotors are cams, gears, flywheels, impellers and grinding wheels as shown by Figure 7. For such rotors, static balancing is used. In static balancing, the unbalanced forces resulting from the acceleration of the unbalanced masses within the system are of concern. To balance a system statically, the sum of all the forces acting on the moving system should be zero. Since the mass of the rigid rotor can be assumed to act in a plane, static balancing can be considered as a single-plane balancing technique. Figure 5 shows the presence of unbalanced masses m_1 and m_3 at two different radii r_1 and r_3 and the addition of mass m_2 at r_2 to balance the centrifugal forces in the plane shown.

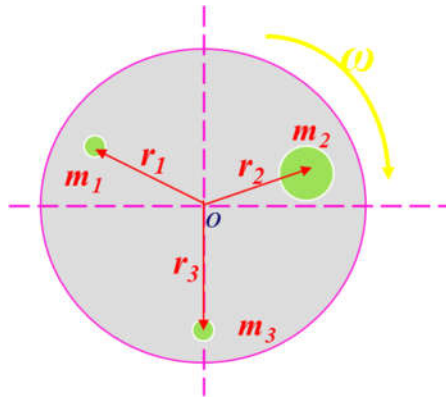


Figure 5: In-plane Balancing

Dynamic balancing is used for non-planar rotors like cam shafts and requires balancing in two planes unlike static balancing which is essentially a two-dimensional balancing technique. It requires that the two following equations are satisfied in the two planes the balancing is done as shown by Figure 6:

$$\sum M = 0$$

Equation 3

$$\sum F = 0$$

Equation 4

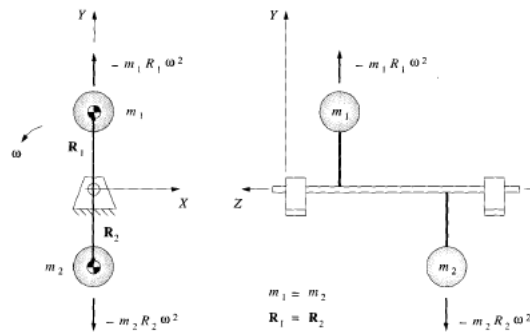


Figure 6: Dynamic Balancing²

² Image obtained from: 8. Norton, R.L., *Design of machinery: an introduction to the synthesis and analysis of mechanisms and machines*. 2004: McGraw-Hill Professional.

Earlier, the necessity for balancing has been established. Since, automobile disk brakes fall into the category of disks, they must undergo static or one-plane balancing. The most commonly used static balancing machines rotate the rotors at high speeds and measure the vibrations associated with it. The unbalanced mass is located where the centrifugal force registers a spike – accelero-gyro sensors placed on the shaft rotating the disk are constantly acquiring vibration data from the rotor.

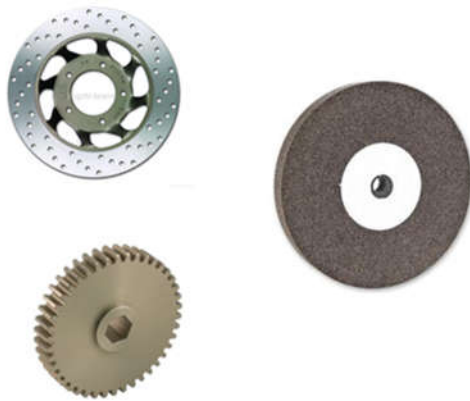


Figure 7: Disk Brake (Top), Gear (Bottom) and Grinding wheel (Right)

This is an effective way of detecting very small amounts of unbalance as increasing the rotations speed will amplify the vibrations by the square of the speed as indicated by Equation 5.

$$mrw^2 = Uw^2 = F \quad \text{Equation 5}$$

This is again reiterated by Figure 8 which shows the force experienced by the rotors as the speed increases.

Several companies exist which continue to provide solutions in rotational balancing technologies like JP and Hoffman. Although very precise and accurate in their operation, these machines often provide a lot more functionalities than are required by the local

industry and therefore, are much costlier to purchase. BVW(F1-F3) designed by Hoffman[9] are multi-stationed balancing machines that boast a resolution of 10gmm, which is far too precise than the 1300gmm limit set by our industrial collaborator. The machine's wide array of functionalities includes inlet conveyor, unbalance measurement, milling unit, automatic separation and swarf extractor among other things. Similar trend can be seen in the products offered by leading balancing machine manufacturers. Shenck's machine has a resolution as fine as 4gmm and allows auto-loading and balancing of rotors with different diameters.

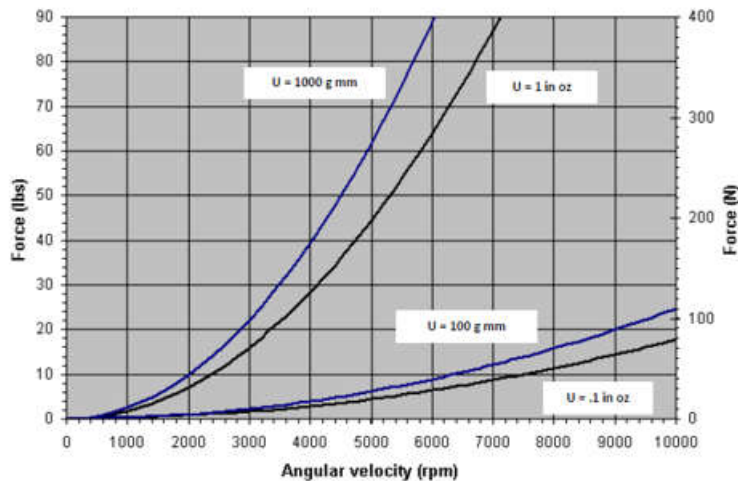


Figure 8: Force against angular velocity for different amounts of unbalance mass³

However, as the data sheets of these products detail, the rotational speeds are very high. BVW11 of Hoffman and V series of CEMB for instance, recommend a speed of 600-800rpm. These high rotational speeds can be justified if one looks at the precision of the machines that goes down to 10gmm. Such low amounts of unbalance mass can easily be

³ Graph taken from: 10. Mitchell, G.k.G.J.W.H.B.J., *Basics of Balancing 202*.

detected at high rpms because their impact on the system vibration becomes rather pronounced as speed increases. A clear illustration of which is shown by Figure 8. The safety risk on the other hand is equally high. Should a worker fail to secure the disk in the chuck, the disk will fly off the bed and injure someone critically. Likewise, finger and arm injuries aren't uncommon among operators of such machinery.

To overcome the aforementioned challenges, it was decided to utilize a non-rotational balancing machine design. Although unconventional, some literature was found on such designs. Hoffman had designed a very unique electro-magnetic system which utilized a three axis gimble and an electro-magnet that balanced the unbalanced mass. The amount of current used to achieve a balanced disk is calibrated against the unbalance mass present in the disk. However, the sensor technology used was extremely costly.

Ametek's model 3867 again used a very expensive linear variable differential transducer(LVDT) to make the measurements. Although, the concept was intriguing, the high costs of quality LVDT prohibited us to utilize this concept in the designs. Kato et al.[11] used three load-cells placed along the circumference of the disk to measure the weight distribution and eventually the unbalance and location.

To strike a balance between fine resolution, safety and cost-effectiveness of machine, a design selection matrix was used to determine the feasibility of each design as shown in Table 1. This led way to an innovative technique to measure the unbalance and its location using the much safer non-rotational method employing load-cells. Another added benefit of this technique was the reduced cycle time because it did not require the disk to be first accelerated to a given speed and then bringing it to rest.

Table 1: Design Selection Matrix

Design selection parameter	%	Rotational Design	LVDT Non-Rotational	Load-cell Non - Rotational
Cost	40	40	20	40
Manufacturability	20	20	10	15
Reliability	10	10	-	-
Maintenance	10	5	10	10
Energy consumption	10	0	5	10
Safety	10	0	10	10
	Total	75	>55	>85

Key:
Full marks for best design
Zero marks for worst design

METHODOLOGY

Working of the system

The system operates by processing sensor data fed to LabVIEW through an Arduino Mega over the serial port. Three load cells are placed at equal radial positions 120 degrees apart. The load cells output voltage proportional to the force applied on each of the cells to the Arduino through the use of external 24-bit Analogue to Digital Converters. Short protected wires along with high frequency signal rejecters work to reduce fluctuation in readings due to random error. The load cells had been calibrated against known masses beforehand, to under 0.5 grams of accuracy. These readings are interfaced to LabVIEW over the serial port in string format and used to obtain the load on the sensors. Spherical balls are placed between the load cells and the disk to ensure point contact. The force values are repeatedly measured and only stable values are stored in the system. Then any change in the stable value may be displayed as loading or unloading of the brake disk. This is done using three layers of shift registers. This change corresponds to when the disk is placed on the cells and when it is removed. The individual cell values are processed to obtain the mass distribution of the disk. Afterwards, summation of moment equations at various positions with a bit of trigonometry gives us the imbalance magnitude and angular position.

A major concern was how to place the disk in such a manner that every time its center would coincide with the center of the system. To do this, we employed a centering cone that would rise and descend in a vertical path that would enable repeatability in the placement of the disk. This movement of the cone was controlled by a linear actuator, controlled through the LabVIEW Front Panel. A control button which would latch till read once was added, and using a combination of a shift register and a timing based conditional command structure, we were able to actuate the cone first downwards so that the disk could be placed on the cells, and then upwards so that it could be removed. Force values were

read upon the disk being removed as opposed to when being placed, as it removes the effect of the impact force due to the momentum of the disk.

All of the previous discourse is based on the assumption that the system was fabricated without any significant manufacturing errors. This unfortunately was not the case. Differences in the side lengths of the triangle formed by the load cells and misalignment of the cone itself with the center of the system necessitated compensation of the imbalance value that ensued. Thus, repeated experimental runs were conducted for the disk at various angular positions and the eccentricity of the cone from the center of the load cells was determined and eliminated by calibration. The process of removing the effect of eccentricity of the system due to manufacturing inaccuracy was also automated. Thus, a button for “Auto-Calibrating” the machine was introduced, which would measure the imbalance measured with a master disk and use the results to compensate the systems own contribution to the imbalance measured for other test disks. In addition, being a vertical protrusion from the actuator, the cone and the shaft it was mounted to experienced horizontal play in the order of up to a millimeter. In order to restrict any horizontal change in the position of the shaft, a linear bearing with a tolerance of $\pm 0.02\text{mm}$ was bolted to the frame. As a result, the system reads zero for a master disk, while otherwise, it indicates the imbalance mass and angle to 130 gmm (± 1 gram) of accuracy for a confidence interval of 90%. Angle markings on the top cover allow easy marking of the imbalance position on the disk. The graphical user interface not only allows the user to control the testing procedure using buttons on a touch screen, it also displays the results in the form of a dial gauge for the angle and fill meter to show the magnitude of the imbalance.

Mathematical equations and resulting imbalance

Derivation of equations:

By $\sum M_y = 0$ whereby the axis is located at the

Centre of the Disk, we get:

$$F_2 \times r \sin(60) + mg \times r \sin(\theta) = F_3$$

$$\sin(\theta) = \frac{(F_3 - F_2) \sin(60)}{mg}$$

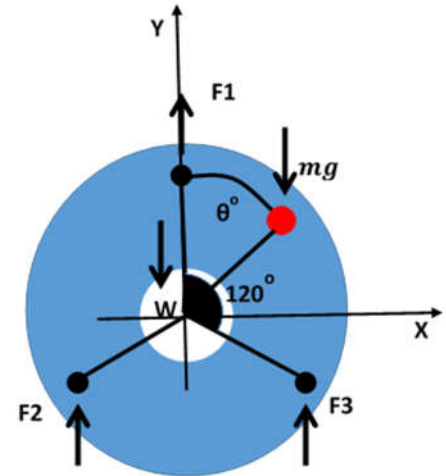


Figure 9: Free Body Diagram of Disk Brake

Equation 6

By $\sum M_x = 0$ whereby the axis is located at the Centre of the Disk, we get:

$$W \times r + mg \times r(1 - \cos(\theta)) = (F_2 + F_3) \times r(1 + \cos(60))$$

Equation 7

By substituting: $W + mg = F_1 + F_2 + F_3$

$$\cos(\theta) = \frac{F_1 - 0.5(F_2 + F_3)}{mg}$$

Equation 8

Using the identity: $\cos^2(\theta) + \sin^2(\theta) = 1$,

$$m = \sqrt{\frac{0.75(F_3 - F_2)^2 + (F_1 - 0.5(F_2 + F_3))^2}{g^2}}$$

Equation 9

Manufacturing Eccentricity Compensation

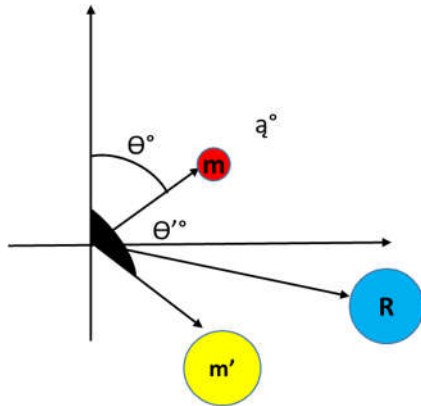


Figure 10: Resultant imbalance due to eccentricity

By Law of Vector Addition:

$$R\cos(\alpha) = m' \cos(\theta') + m\cos(\theta)$$

$$m\cos(\theta) = R\cos(\alpha) + 221.3$$

Equation 10

$$R\sin(\alpha) = m' \sin(\theta') + m\sin(\theta)$$

$$m\sin(\theta) = R\sin(\alpha) - 102.7$$

Equation 11

Using the identity: $\cos^2(\theta) + \sin^2(\theta) = 1$,

$$m = \sqrt{(R\sin(\alpha) - m' \cos(\theta'))^2 + (R\cos(\alpha) - m' \sin(\theta'))^2}$$

Equation 12

Load cell uncertainty

Uncertainty in a reading is a critical factor for any problem in the field of instrumentation, particularly as it defines not only the expected variation of the reading from its true value and its level of precision, but also represents the degree of confidence the end user may hold on the results. Knowledge of repeatability characteristics of the instrument is of paramount importance for the user when making the most informed decisions.

Uncertainty value has been quantified by the use of load cell data sheet made available in Appendix III. Below is a brief summary of the uncertainty parameters in the machine, backed with validation from experimental results. The load cells in use have a maximum load of 5 Kg.

Discrimination Threshold:

Discrimination threshold is the minimum change in the output of the load cell that would cause any visible change in the results displayed. This is a value set by the programmer, so as to avoid garbage readings due to signal noise, external vibrations, or very light disturbances to be displayed on the screen. For the purpose of this project, a discrimination threshold of **0.5 grams** has been used.

Zero balance:

Zero balance of a load cell can reach as high as 2% full scale which translates to 100 grams. Although, such high deviations were not observed during experimental testing of the load cells, this offset error can be minimized by taking a difference between two output readings.

Linearity:

Linearity tells us how closely the readings from a load cell adhere to their line of best fit. As mentioned in the datasheet, the error in linearity is less than 0.005%. This translates to an error of **0.25 grams**, full scale. Non-linearity can be minimized by calibrating the load cells over a window range of its application.

Response Time:

Response time, as seen by experimentation is quite fast, in the range of milliseconds. At the moment, further investigation into the response time is neither feasible nor required.

Repeatability:

Repeatability refers to how close the readings obtained are when taken under identical conditions. The datasheet defines the error in repeatability to be within 0.005% of the full scale, which is 0.25 grams. Under identical conditions, and as validated within a common time window of 20 minutes, results have shown to vary up to 0.4 grams.

Temperature:

Effect of varying temperatures effect load cell output reading up to 0.005% per 10°C. With expected variation of 20°C, the variation translates to **0.5 grams**. However, the experimental results show temperature based variation up to 3 grams per load cells. It must be noted that all three load cells are expected to behave similarly to temperature variation and thus will result in a zero balance offset that can be minimized by taking difference between two output readings.

The error from the aforementioned uncertainties resulted in limited precision of the system. The combined effect of these uncertainties was checked experimentally by varying external conditions and setting up control experiments. A large number of readings were noted to evaluate the expected uncertainty of the whole system which is discussed further in the results section.

Coding flowchart

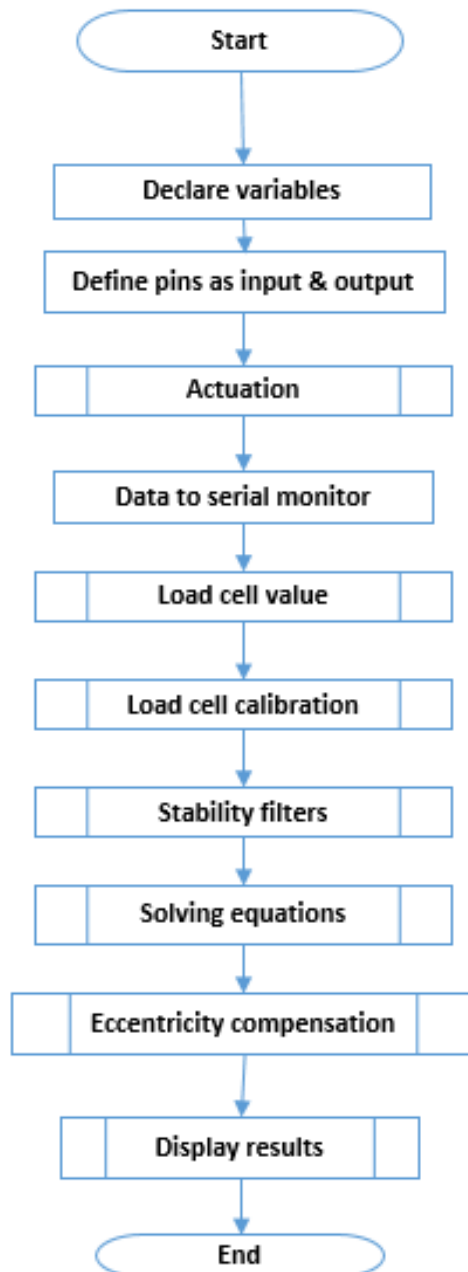


Figure 11: coding steps

RESULTS AND DISCUSSION

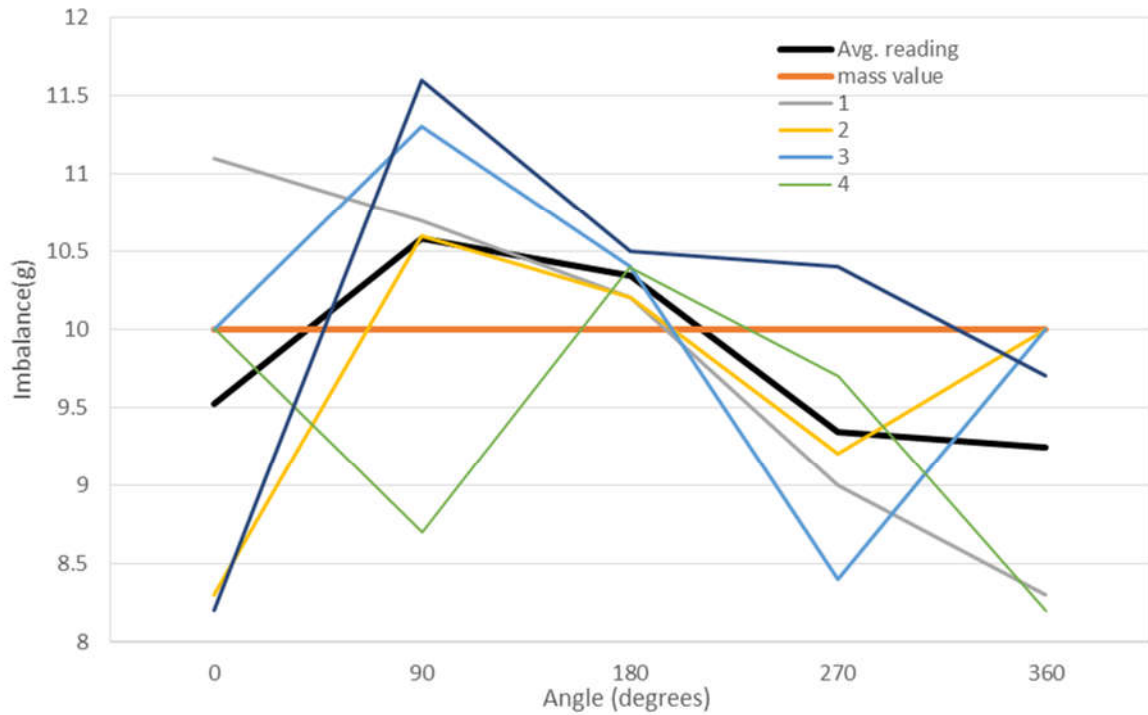


Figure 12: Unbalance values at different locations of known mass

A known value of 10g unbalance was positioned at four different bearing positions and the results given by the machine are displayed in Figure 12. A similar analysis was conducted to determine the degree of accuracy with which the machine located the unbalance as shown by Figure 13. The lines labeled 1 – 5 are the different sets of readings used to check for the repeatability of the system. When a mass of 10g is added at different orientations on the disk, the reading shows a maximum error of ± 2 g. Analyzing the trend over all the sets reveals a pattern between the error and the location of unbalance. Overall, at bearings of 90° and 180° , a positive bias is observed and at 270° a negative bias can be seen with the value at 0° showing variation on either side of the 10g. This can primarily be associated

with any manufacturing errors within the system; the load-cells are displaced by a fraction under a millimeter from their design location. Quite similar trends are observed in the bearing indicated by the machine. A maximum error observed was of $\pm 13^\circ$ as shown by Figure 13.

Note that the system doesn't make any explicit measurements regarding the location and amount of the unbalance. It only calculates these values from the weight distribution data fed into LabVIEW from the sensors. So even though the error in an individual load cell reaches a maximum of $\pm 0.5\text{g}$, the error in the unbalance and bearing gets compounded as several uncertainties combine together to give the final output.

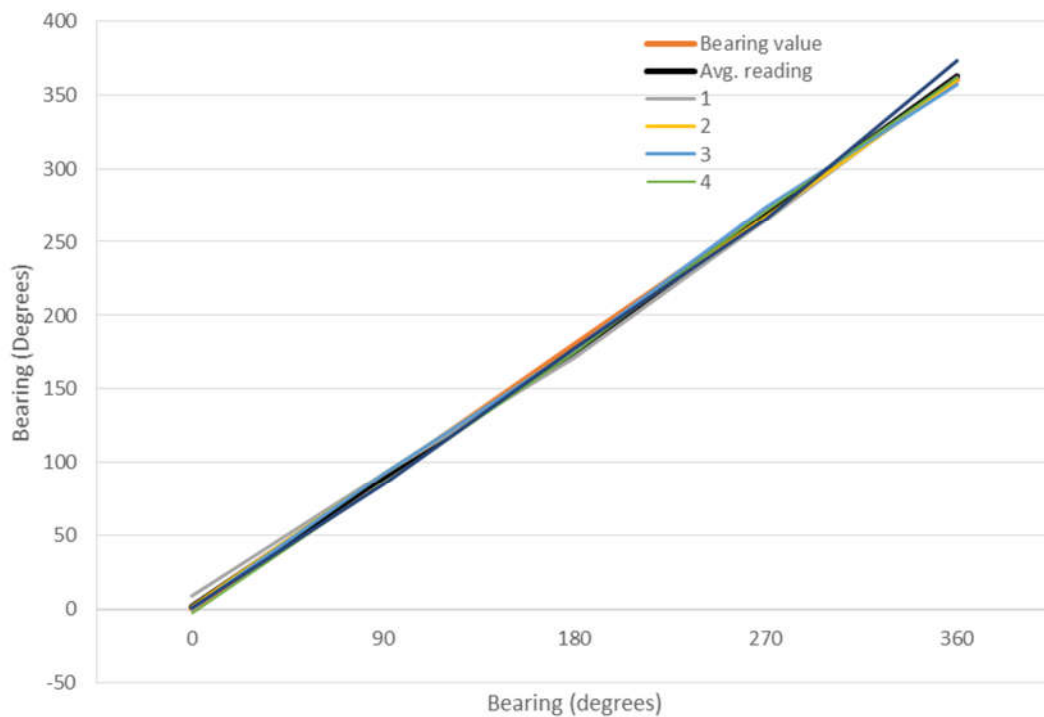


Figure 13: Comparison of bearing given by machine with a known bearing

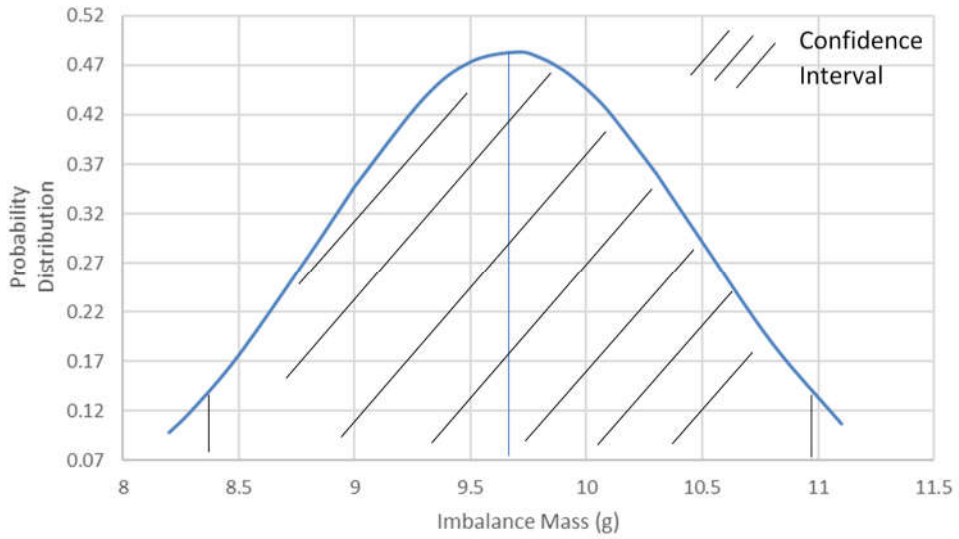


Figure 14: 90% Confidence Interval for the amount of unbalance

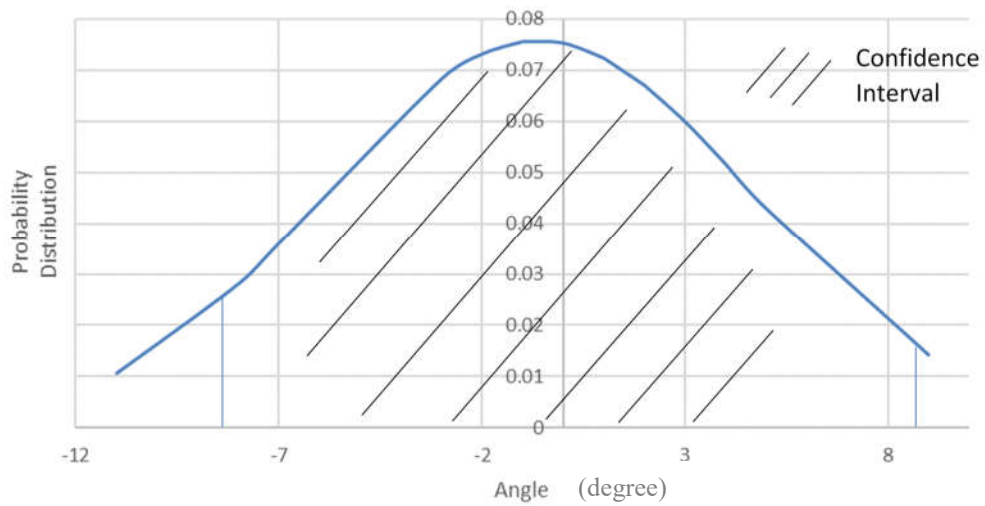


Figure 15: 90% Confidence Interval for the location of unbalance

Extensive trials provided a good normal distribution of data for both the unbalance and its location as shown by Figure 14 and Figure 15. It is reminded that the maximum deviation permitted is a touch under 10g. The accuracy of this system is well within the acceptable bounds. 90% of the data for the unbalance amount and the bearing lie within the following ranges respectively:

$$8.38g < m < 10.98g$$

$$8.8^\circ < \theta < 8.4^\circ$$

The design matrix, represented by Table 1 details the importance of cycle time and maintenance costs incurred for this machine. Industrial settings need quick progression of products from the products through the multitude of processes to prevent any holdups and enhance inventory turnover rate. While rotational machines take 20-30seconds for one cycle, this machine performs the same task within 10-15s. Thereby, providing operators to increase number of disks tested per minute to 4-6 from 2-3 on the rotational platforms. Moreover, a rotational balancing machine on average is operated by a 1.5kW whereas this innovative design only consumes about 150 W. The power consumption of a rotational one is ten times more than that of a non-rotational one.

CONCLUSION AND RECOMMENDATION

Design of a non-rotational automobile disk brake balancing machine was carried out after critical evaluation of all other options available. A cost-benefit analysis between three different designs based on accuracy achievable, safety, cost of manufacturing and power consumption was carried out and a non-rotational machine employing three equally spaced load-cells was chosen as the optimum concept that met all of the aforementioned criteria at a very economic rate. Interfacing of the hardware was done with LabVIEW and a graphical user interface is also included within the package to enhance user experience.

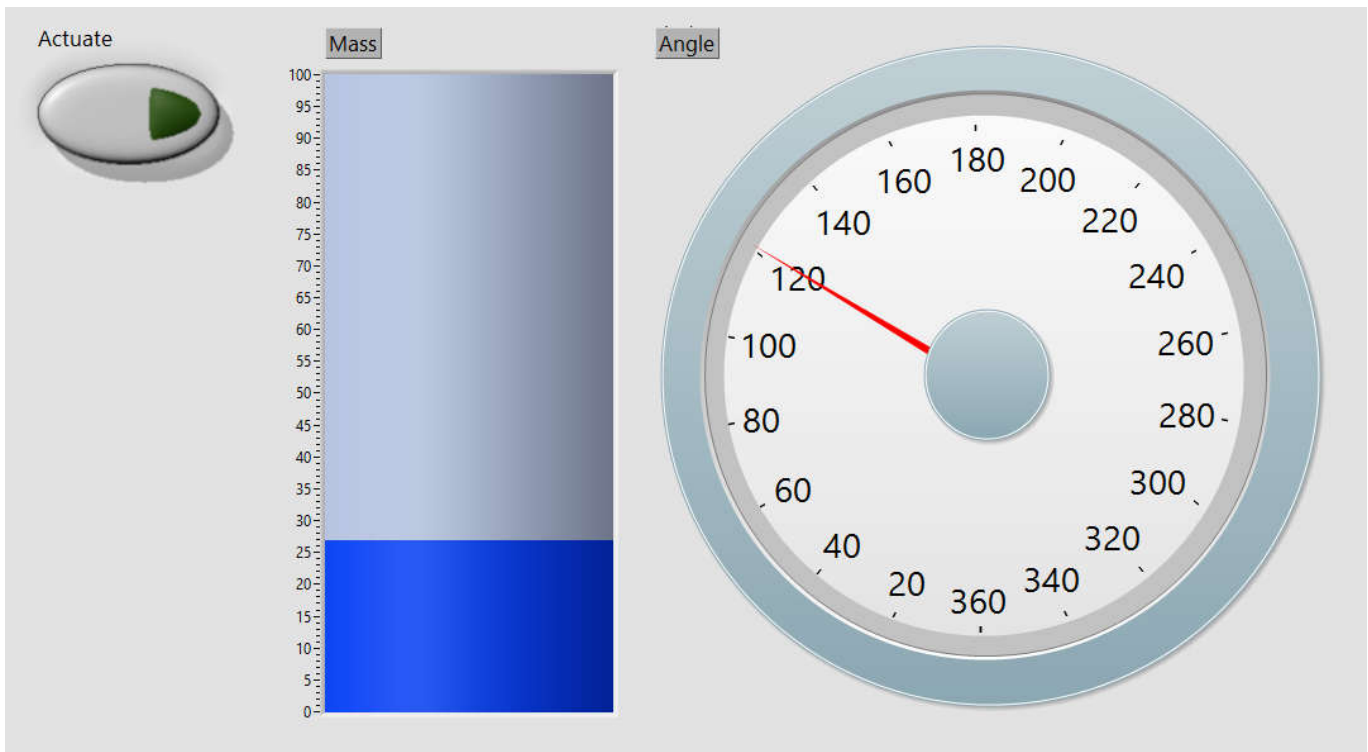
This project was done in collaboration with MECAS Engineering who are the industry partners and sponsors of this project. A proof of concept was prepared in accordance with the request of MECAS Engineering, which is in the process of expanding its product line and has shown great interest in the project, especially after the results of the machine are within the acceptable bounds detailed by MECAS Engineering.

It is recommended to take this project a step further and deliver a commercialized product with industrial grade fabrication quality. Further improvements in this machine mainly constitutes the use of high quality load sensors to achieve better precision and repeatability. The machine can also be coupled with an unbalance correction mechanism such as grinding the disks to remove mass at detected location.

REFERENCES

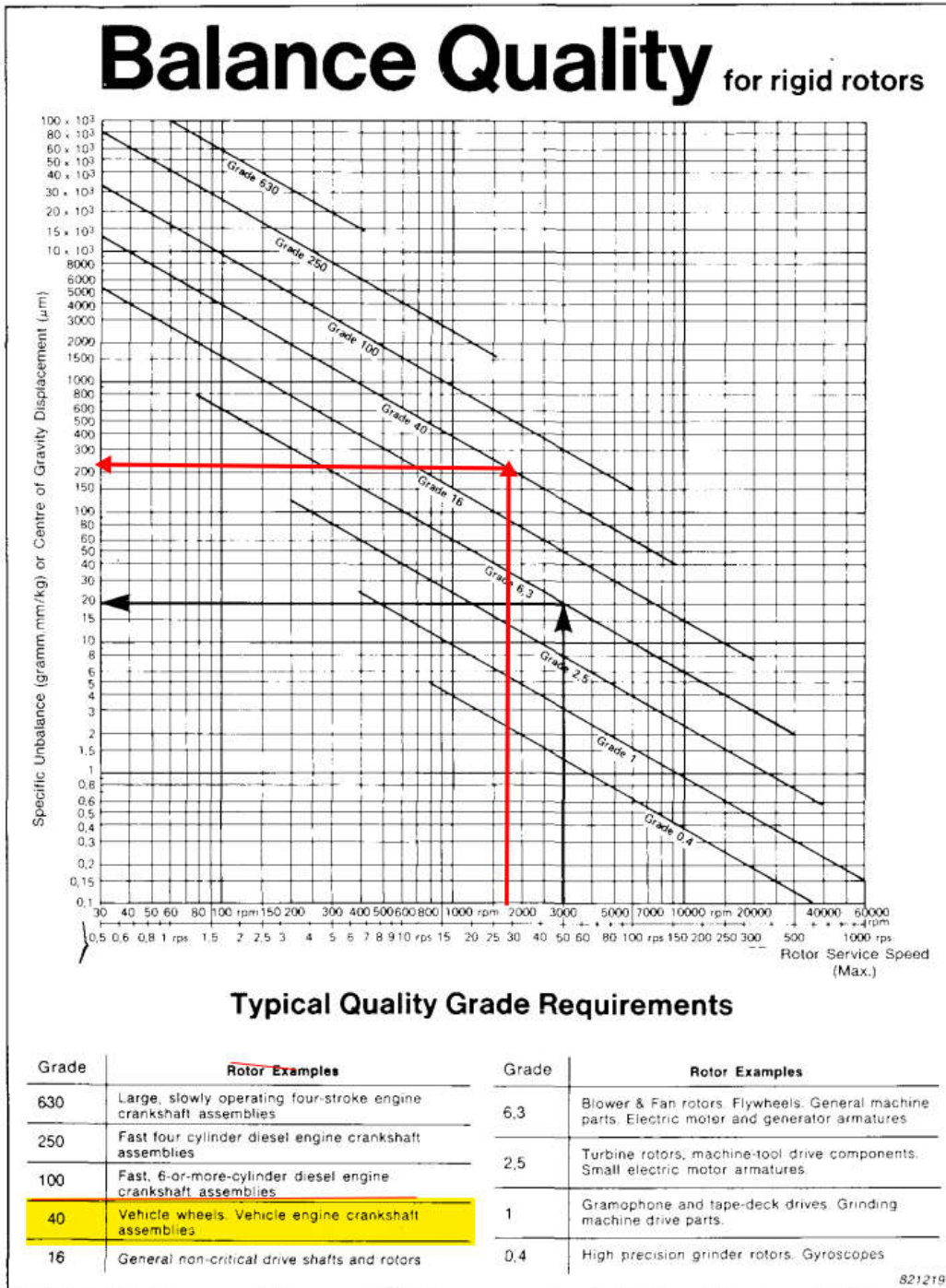
1. Mackin, T.J., et al., *Thermal cracking in disc brakes*. Engineering Failure Analysis, 2002. **9**(1): p. 63-76.
2. Trebuña, P., et al., *The analysis of failure causes of the rotor shaft of steam turbines*. Metalurgija, 2017. **56**(1-2): p. 233-236.
3. Boniardi, M., et al., *Failure analysis of a motorcycle brake disc*. Engineering Failure Analysis, 2006. **13**(6): p. 933-945.
4. Tian, Y., et al. *Analysis of Vibration Failures Caused by Imbalanced Mass of Machinery under High Speed Rotation*. in *2011 Asia-Pacific Power and Energy Engineering Conference*. 2011.
5. Tu, Y., J. Zakrajsek, and D. Townsend, *Effects of gear box vibration and mass imbalance on the dynamics of multistage gear transmission*. Journal of Vibration and Acoustics, 1991. **113**: p. 333.
6. Beatty, R.F., *Differentiating Rotor Response Due to Radial Rubbing*. Journal of Vibration, Acoustics, Stress, and Reliability in Design, 1985. **107**(2): p. 151-160.
7. Shortle, J.F. and M.B. Mendel, *Predicting dynamic imbalance in rotors*. Probabilistic Engineering Mechanics, 1996. **11**(1): p. 31-35.
8. Norton, R.L., *Design of machinery: an introduction to the synthesis and analysis of mechanisms and machines*. 2004: McGraw-Hill Professional.
9. Hofmann, *BVW-11, Balancing Machines for Brake Disks*.
10. Mitchell, G.k.G.J.W.H.B.J., *Basics of Balancing 202*.
11. Kato, S. and T. Aikawa, *Device for measuring the imbalance of an object*. 1984, Google Patents.

APPENDIX I: LABVIEW USER INTERFACE



LabVIEW user interface showing imbalance amount in grams and location in degrees with a latch to initiate the detection cycle.

APPENDIX II: ISO STANDARD REFERENCE



Disk Brakes can be classified as Grade 40 rotors as per ISO 1940 balancing standards.

At 120 mph speed of automobile, disk brake rotates at 1680 rpm, requiring 220 gmm/kg.

With total mass of disk around 6.2 kg, unbalance to detect totals to 1350 gmm.

Thus, the precision of machine was kept as such that it detects the required 1300 gmm.

Figure 16: Briel & Kjaer Unbalance Nomogram, based on ISO quality standards.

APPENDIX III: LOAD CELL DATA SHEET

Product Name	Weighing Load Cell
Rated Load	0-5Kg
Rated Output	1.0946mV/V
Linearity	=<0.005%F.S
Hysteresis	=<0.005%F.S
Repeatability	=<0.005%F.S
Zero Balance	±2%F.S
Temp Effect on Zero	=<0.005%F.S. 10°C
Temp Effect on Zero Output	=<0.005%F.S. 10°C
Creep	=<0.005%F.S./30minu
Corner Error	±1uV
Input Impedance	410±10Ω
Output Impedance	350±3Ω
Insulation	>5000MΩ/50V DC
Compensated Temperature Range	-10°C~40°C
Operating Temperature Range	-20°C~60°C
Safe Overload	150%F.S.
Ultimate Overload	200%F.S
Input End	Red+, Black-
Output End	Green+, White-
Test Instrument	E2000
Force Testing Equipment	Actual Load
Excitation Voltage	5-10V DC
Total Size	8 x 1.3 x 1.3cm / 3.1" x 0.5" x 0.5"(L*W*T)
Thread Hole Diameter	Big: 4mm / 0.157" Small: 3mm / 0.118"
Center Hole Distance	1.8 x 1.1cm / 0.708" x 0.433"(L*Radius)
Cable Length	21cm / 8.3"
Weight	30g
Package Content	1 x Weighing Load Cell

APPENDIX IV: BILL OF MATERIALS

Item No.	Item name	Cost
1	T-iron	150
2	L-iron	1450
3	Sheet metal	1870
4	Acrylic transparent	500
5	bolts/washers	220
6	lathe drill/thread	300
7	welding frame	500
8	Fuel sadar	100
9	drill bits	50
10	inches tape	60
11	evs lights/cable	350
12	taxi sadar	350
13	Angle L + cutting	1620
14	chrome spray	170
15	drilling	150
16	drill key	70
17	frame welding	1000
18	washer	10
19	Acrylic black	340
20	Laser cutting	300
22	nut bolt	30
23	sheet metal hole	100
24	sheet metal hole	100
25	Fuel	200
26	hinge/bit	200

27	nut bolt	50
28	hinge bolt	20
29	acrylic smoke	840
30	laser cutting	300
31	frame casing	4200
32	cone metal	805
33	relay/load cell	1480
34	load cell small	950
35	angle iron	200
36	bolts	70
37	metal plate	1000
38	load cells	3000
39	wires	890
40	bearing	550
41	report print	264
42	printing 2	70
43	print 3	170
44	shaft	2320
45	fuel	150
46	Acrylic + laser	800
47	switch + elfi	200
48	Arduino	1300
49	Brochure	700
50	Standee	500
51	Bike repair	100
52	Fuel UZ car	200
53	Actuator	15000
Total		46319